AIP | Physics of Plasmas

Angle-dependent modulated spectral peaks of proton beams generated in ultrashort intense laser-solid interactions

L. N. Su, Z. D. Hu, Y. Zheng, M. Liu, Y. T. Li, W. M. Wang, Z. M. Sheng, X. H. Yuan, M. H. Xu, Z. W. Shen, H. T. Fan, L. M. Chen, X. Lu, J. L. Ma, X. Wang, Z. H. Wang, Z. Y. Wei, and J. Zhang

Citation: Physics of Plasmas (1994-present) **21**, 093111 (2014); doi: 10.1063/1.4896338
View online: http://dx.doi.org/10.1063/1.4896338
View Table of Contents: http://scitation.aip.org/content/aip/journal/pop/21/9?ver=pdfcov
Published by the AIP Publishing

Angle-dependent modulated spectral peaks of proton beams generated in ultrashort intense laser-solid interactions

L. N. Su,[1] Z. D. Hu,[1] Y. Zheng,[1] M. Liu,[1] Y. T. Li,[1,a)] W. M. Wang,[1] Z. M. Sheng,[2,3] X. H. Yuan,[2] M. H. Xu,[4] Z. W. Shen,[1] H. T. Fan,[1] L. M. Chen,[1] X. Lu,[1] J. L. Ma,[1] X. Wang,[1] Z. H. Wang,[1] Z. Y. Wei,[1] and J. Zhang[2,b)]
[1]*Beijing National Laboratory for Condensed Matter Physics, Institute of Physics, Chinese Academy of Sciences, Beijing 100190, China*
[2]*Key Laboratory for Laser Plasmas (MoE) and Department of Physics and Astronomy, Shanghai Jiao Tong University, Shanghai 200240, China*
[3]*Department of Physics, SUPA, University of Strathclyde, Glasgow G4 0NG, United Kingdom*
[4]*Department of Physics, China University of Mining and Technology (Beijing), Beijing 100083, China*

(Received 27 June 2014; accepted 9 September 2014; published online 24 September 2014)

Proton acceleration from 4 μm thick aluminum foils irradiated by 30-TW Ti:sapphire laser pulses is investigated using an angle-resolved proton energy spectrometer. We find that a modulated spectral peak at ~0.82 MeV is presented at 2.5° off the target normal direction. The divergence angle of the modulated zone is 3.8°. Two-dimensional particle-in-cell simulations reveal that self-generated toroidal magnetic field at the rear surface of the target foil is responsible for the modulated spectral feature. The field deflects the low energy protons, resulting in the modulated energy spectrum with certain peaks. © *2014 AIP Publishing LLC*. [http://dx.doi.org/10.1063/1.4896338]

I. INTRODUCTION

Laser-driven ion beams have advantages of short pulse duration, high brightness, and small source size. For their potential applications such as proton radiography,[1] proton-driven fast ignition,[2] tumour therapy,[3] proton-driven nuclear reactions,[4] etc., monoenergetic spectral distributions of protons are preferred. However, most of the experimentally generated proton beams present exponential-like proton energy spectra. To produce proton beams with modulated spectral distributions, several mechanisms, such as radiation pressure acceleration,[5] break-out afterburner,[6] and laser-driven shock acceleration,[7] have been proposed and successfully demonstrated by numerical simulations and experiments.[8,9] However, to implement these mechanisms, the drive laser pulses must have very high contrast ratio better than 10^{-10} and high focused intensity higher than 10^{21} W/cm^2, typically. Such requirements are great challenges for the laser systems in commission.

With the current laser parameters, the target normal sheath acceleration (TNSA) has been the typical mechanism found in experiments for laser-driven ion acceleration.[10,11] How to generate proton beams with modulated spectral distributions by TNSA mechanism has been investigated by many groups in the last decade. In the interaction of a 20-TW/0.8 ps laser with a hydrogen-desorbed palladium foil target, Hegelich *et al*. obtained a spectrally modulated C^{5+} ion beam by removing the contaminants on the target rear surface.[12] Schwoerer *et al*. reported quasi-monoenergetic protons emitted in the target normal direction from microstructured targets with a 10 TW Ti:sapphire laser.[13] Toncian *et al*. used ultrafast laser-driven micro lens to focus MeV protons with specific energies, generating modulated proton beams.[14]

Based upon the target manipulation, Robinson *et al*. observed quasi-monoenergetic proton beams in the target normal direction from 50–200 nm planar foil targets irradiated by the ASTRA Ti:sapphire laser pulses.[15] From particle-in-cell (PIC) simulations, they find two self-generated toroidal magnetic fields at the rear surface of the ~nm ultrathin foil. The field near the target center will focus protons, while the field a little far from the target center will deflect protons off the target normal direction. According to their explanation, the focusing field can self-select protons with certain energies, leading to the spectral peaks. For micron-thickness targets, the focusing field will disappear and no spectral peaks are observed in the normal direction.

In this paper, we will present our observation of proton beams emitted from micron-thickness foils irradiated by 30-TW Ti:sapphire laser pulses by using an angle-resolved magnetic spectrometer. We find that modulated spectral peaks are presented at 2.5° *off* the target normal direction for 4 μm thick aluminum foil targets. Our PIC simulations show that a strong toroidal magnetic field is also generated at the rear target surface. This field will deflect (rather than focus) the low energy protons away and make the protons with certain energies outstanding.

II. EXPERIMENTAL SETUP

The experiment was conducted on the Xtreme Light (XL) Ti:sapphire laser facility at the Institute of Physics, Chinese Academy of Sciences.[16] The schematic setup is shown in Fig 1. A *p*-polarized laser pulse of 100 fs pulse duration, 800 nm central wavelength was focused using an *f*/1.67 off-axis parabola (OAP) mirror onto target foils at an incidence angle of 15°. The laser energy on target after

a)Electronic mail: ytli@aphy.iphy.ac.cn
b)Electronic mail: jzhang1@sjtu.edu.cn

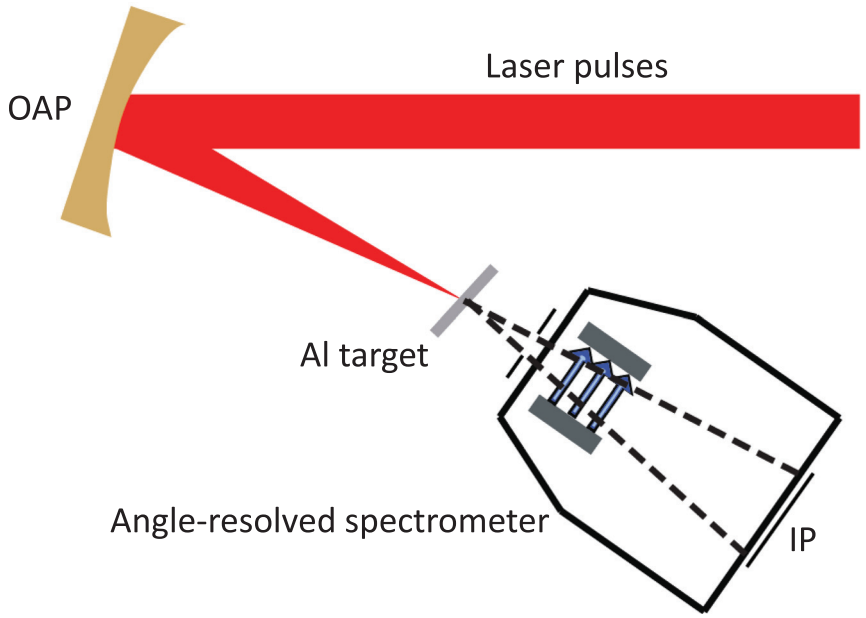

FIG. 1. Experimental schematic. A *p*-polarized laser pulse was focused by an *f*/1.67OAP mirror onto a 4 μm aluminum foil at an incidence angle of 15°. The FWHM of the laser focal spot is 8 μm, giving the maximum laser intensity up to 5×10^{19} W/cm^2. The protons generated from the target are measured by an angle-resolved proton energy spectrometer. Using a horizontal lead slit as an entrance, the spectrometer can collect the protons within the laser propagation direction and the target normal direction.

compression could be adjusted from 1 to 2.5 J. The full width at half maximum (FWHM) of the laser focal spot was 8 μm, giving a maximum laser intensity of 5×10^{19} W/cm^2. The contrast ratio at 7 ns before the main laser pulse was better than 10^{-6}. The targets were 4 μm-thick aluminum foils.

An angle-resolved proton energy spectrometer[17] was set at 8 cm away from the target. A 30 mm × 0.2 mm horizontal lead slit was used as an entrance of the spectrometer. A slowly varying magnetic field with central field strength of 0.3 T was applied to disperse the protons. The spectrometer could collect the protons emitted into the angle range of 16°, which covered both the laser propagation (LP) direction and target normal (TN) direction. The vertical collection angle was 2.5 mrad. The detector was 98 mm × 49 mm calibrated TR-imaging plates (IPs). The resolution of the IP scanner is 50 μm. The angular resolution of the spectrometer was 0.14°, determined by the slit width and the scanner resolution. A 4 μm thick aluminum filter was used to cover the imaging plates to block the carbon ions with energies less than 4 MeV. In the present experiment, we found that the carbon ions with energies higher than 4 MeV were not measurable. This was confirmed by using a traditional Thomson parabolic spectrometer with a pinhole as an entrance.

III. RESULTS AND DISCUSSIONS

A typical proton image on the imaging plate obtained for a 4 μm-thick Al target is shown in Fig. 2(a). The red line on the top of the image is formed by photons and neutral particles directly through the entrance slit, which can be used as the original points for the proton spectra. The vertical and horizontal directions correspond to the proton energy dispersion and angular distribution, respectively. We define θ to be the angle respect to the target normal direction. $\theta = 15°$ corresponds to the laser propagation direction. Note that the large distance between the two magnets leads to the magnetic field profile to be a Gaussian-like distribution, which results in the curved top edge of the proton image. This has been corrected when deducing proton spectra.

From Fig. 2(a), we can see the proton spectra are angle-dependent. We plot the proton spectra in the target normal direction ($\theta = 0°$) and laser propagation ($\theta = 15°$) in Figs. 2(b) and 2(c), respectively. For the target normal direction, the proton cut-off energy is 1.2 MeV and the temperature is 0.23 MeV. For the laser propagation direction, the proton cut-off energy is 1.26 MeV, and the average temperature is 0.31 MeV. There are no modulated peaks presented in both directions.

An interesting feature in Fig. 2(a) is the presence of a yellow ellipse in the energy range from 0.51 to 0.75 MeV and the angle range from 0.5° to 4.3° off the target normal direction, marked by a black dashed circle. Proton counts per unit area in the yellow ellipse are obviously less than those in the surrounding regions, so that there should be spectrally modulated distributions presented around the ellipse. A similar structure is also observed previously.[17] The proton energy spectra in the middle ($\theta = 2.5°$) and the right side ($\theta = 1.2°$) of the ellipse are shown in Figs. 2(d) and 2(e), respectively. For the middle position, the count of protons with energies of less than 0.76 MeV is obviously less than that in the target normal direction, resulting in the protons at ~0.82 MeV outstanding in the spectrum. The $\Delta E/E$ of the modulated spectral peak is estimated to be 25%. For the right side of the ellipse, the modulated spectral peak is at 0.76 MeV and the $\Delta E/E$ is about 33%. For 2.5°, the proton count at the valley ($E = 0.71$ Mev) is 3.49×10^5; while the proton count at the peak ($E = 0.82$ Mev) is 6.65×10^5. As a result, the depth of the modulation is 48%. Meanwhile, for 1.2°, the depth of modulation is 43%.

In our experiment, the laser incidence angle is 15°, which may induce an asymmetric acceleration field due to the angular separation of resonance absorption and J × B hot electrons. For TNSA, the maximum energy of the proton beam is determined by the strength of the sheath field and

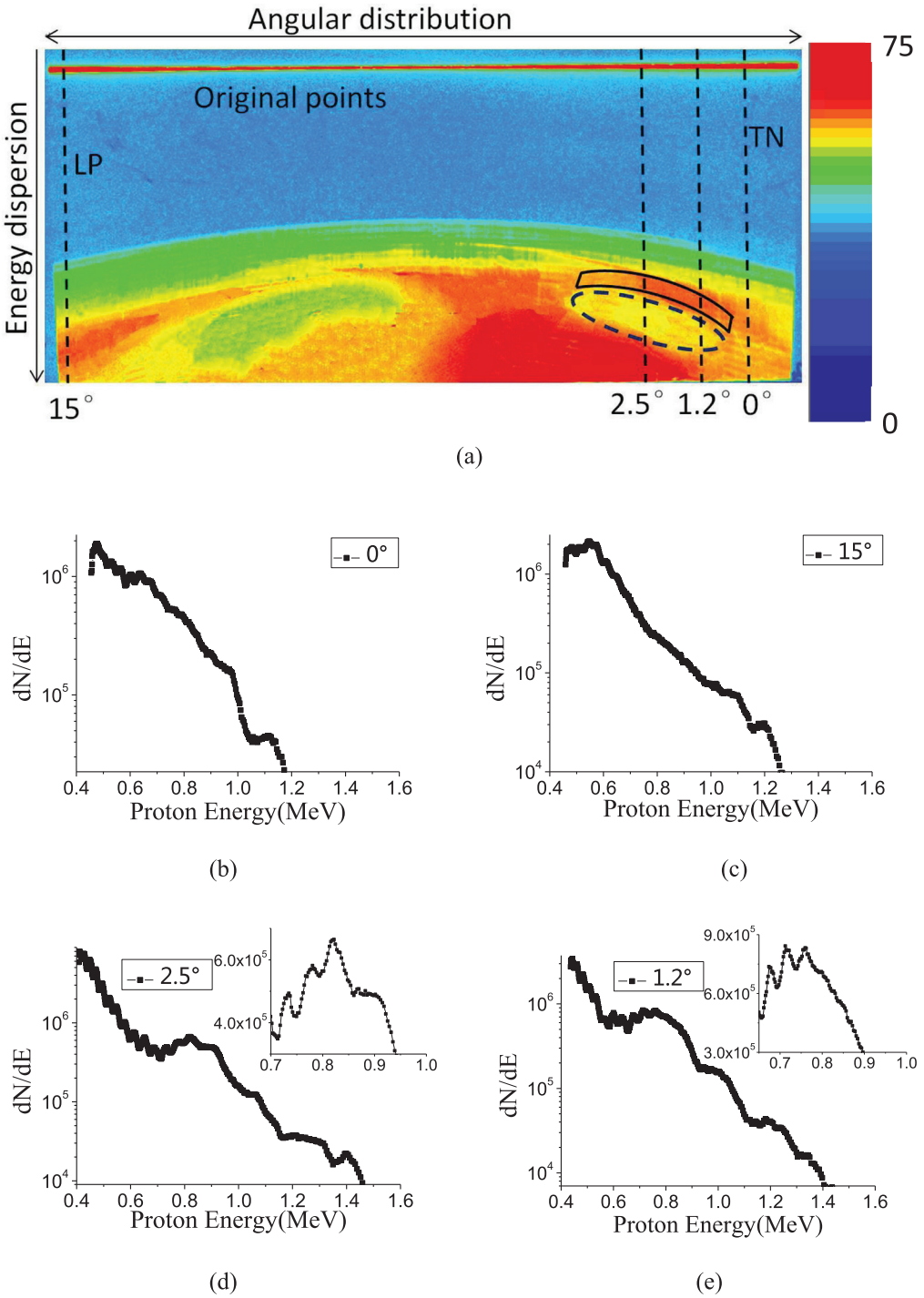

FIG. 2. Raw image of proton signal on the IP detector (a) and the lineout proton spectra in different directions (b–e). Laser energy on target is obtained at 1.9 J. The horizontal and vertical directions of the image correspond to the angular distribution and the energy dispersion of the protons, respectively. Note that there is a yellow ellipse area from 0.5° to 4.3°, where the proton numbers are obviously lower than the surrounding region. This area is marked with a black dashed elliptic circle in (a). The region above the ellipse, marked by a solid black box, shows a spectrally modulated feature. (b–e) The proton spectra for the four typical directions, $\theta = 0°$ (the target normal), 15° (the laser propagation), 2.5° (the middle of the ellipse), and 1.2° (the side of the ellipse), respectively. The insets in (d) and (e) show the spectral peaks in linear ordinate. Proton counts detected by the IP are given per 1 MeV and per 6×10^{-3} msr. Spectral peaks at 0.82 MeV in (d), and at 0.76 MeV in (e) are presented, while no significant spectral peaks in (b) and (c).

the acceleration time, while the emission direction is mainly determined by the normal direction of the local target area. The asymmetric acceleration field may affect the maximum energy of the protons emitted from different local areas. However, it will not lead to a modulated spectral peak at a certain angle. Previous studies show that if the target rear surface is influenced by a prepulse or ASE, the proton beam will be deviated from the initial target normal.[18] However, the prepulse will not lead to a spectrum modulation either.

Ultrafast laser-driven proton radiography shows that a large amplitude (thousands of Tesla) magnetic field is generated at the rear of foil targets irradiated by high-intensity

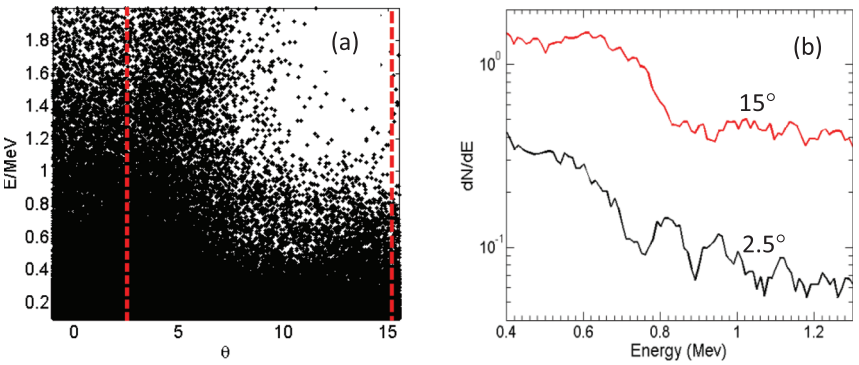

FIG. 3. (a) Simulated proton energy spectra versus emission angle. (b) Simulated spectra of the protons emitted at < 2.5 mrad in the direction of $\theta = 2.5°$ and 15° from the target normal at $t = 300\,\tau_0$. A quasi-monoenergetic peak at 0.81 MeV is presented at 2.5°.

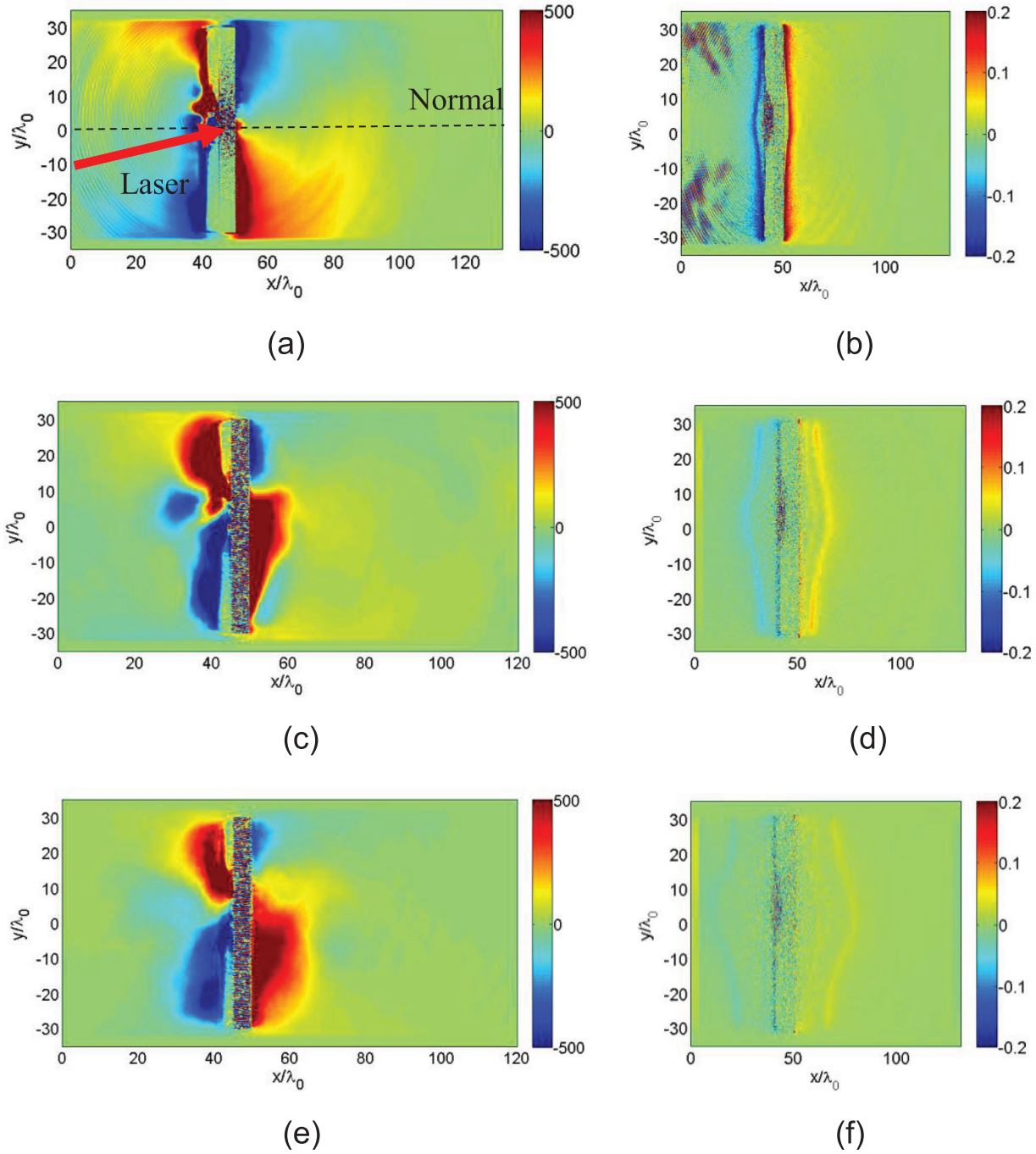

FIG. 4. Distributions of the simulated magnetic fields, B_z, at $t = 100\ \tau_0$ (a), $t = 200\ \tau_0$ (c), and $t = 300\ \tau_0$ (e) and the normalized electrostatic fields, E_x, at $t = 100\ \tau_0$ (b), $t = 200\ \tau_0$ (d), and $t = 300\ \tau_0$ (f). The target is located at the region $40 \le x/\lambda_0 \le 50$, $-35 \le y/\lambda_0 \le 35$. The magnetic field is in unit of Tesla. The magnetic field strength is up to 1000 T.

laser pulse.[19] Robinson *et al.* have found that the self-generated magnetic field plays important role on the presence of the quasi-monoenergetic proton peaks for ultrathin foils.[15] To understand our observation for thick targets, we have carried out numerical simulations by the 2D3V PIC code KLAPS.[20,21] The simulation parameters are similar to the experimental. The temporal and spatial resolutions in the simulations are $dt = 0.025\tau_0$, and $dx = dy = 0.025\lambda_0$, where λ_0 and τ_0 are laser wavelength and laser period, respectively. There are 36 simulation particles in each cell, for both ions and electrons. Absorption boundaries for the fields and particles have been adopted. A Gaussian laser pulse with a normalized vector potential $a_0 = 2.4$ (corresponding to the laser intensity of $2.5 \times 10^{19}\,\mathrm{W/cm^2}$) is incident from the left boundary at an angle of 15°. The target is located at the region $40\lambda_0 \le x \le 50\lambda_0$, $-35\lambda_0 \le y \le 35\lambda_0$. The target consists of a uniform plasma slab with a density of $n_e = 30n_c$ and a preplasma, where n_c is the plasma critical density. The preplasma density profile at the front surface of target follows $n_e(x) = 1.5\gamma_{osc} n_c \exp[(x-40)/2\lambda_L]$, where $\gamma_{osc} = \sqrt{1 + a_0^2/2}$ is the Lorentz factor related to the quiver oscillation of electrons driven by the laser electric field. The preplasma scale length λ_L is set to be $2\lambda_0$.

Simulated proton energy spectra versus emission angle is plotted in Fig. 3(a), $\theta = 2.5°$ and $\theta = 15°$ are marked with red dash lines. The simulated proton spectra emitted into a collection angle of 2.5 mrad in the directions of $\theta = 2.5°$ and $\theta = 15°$ from the target normal are plotted, as shown in Fig. 3(b). We can see a modulated spectral peak presented at 0.81 MeV in the direction of $\theta = 2.5°$. However, there is no modulation in the spectrum in the direction of $\theta = 15°$. This is in good agreement with the observed spectra in Figs. 2(c) and 2(d). In the simulations, a self-generated toroidal magnetic field with strengths 100–1000 T is observed at the rear surface. We plot distributions of the simulated magnetic fields and the electrostatic fields in Fig. 4. According to the Maxwell equations, $B_z^{\cdot} \approx \partial_y E_x$, the target normal sheath field varies transversely with time, generating the toroidal magnetic field in the rear surface of target.[15] The magnetic field is symmetrical at $100\tau_0$, and then becomes more and more asymmetrical at later time. This is associated with the asymmetric electron generation and transport with oblique incidence of the laser pulse.

We track the trajectories of 1% of the total protons with energies higher than 0.2 MeV in the simulations. Their trajectories in momentum space are plotted in Fig. 5, where P_x and P_y are the longitudinal and transverse momentum, respectively. The blue lines correspond to the $E > 0.8$ MeV protons, and the black lines to the $0.2 \sim 0.8$ MeV protons. The $E < 0.8$ MeV protons have large transverse momentum. However, the transverse momentum of the $E > 0.8$ MeV protons is much lower than the longitudinal momentum. This indicates that the low energy protons are much scattered and the high energy protons are directional. The experimental angle-dependent spectral peaks are believed to be caused by the deflection of the protons due to the self-generated magnetic field. Under the influence of the field, most of the $E < 0.8$ MeV protons are deflected out of the collection angle of 2.5 mrad, while the $E > 0.8$ MeV protons are not.

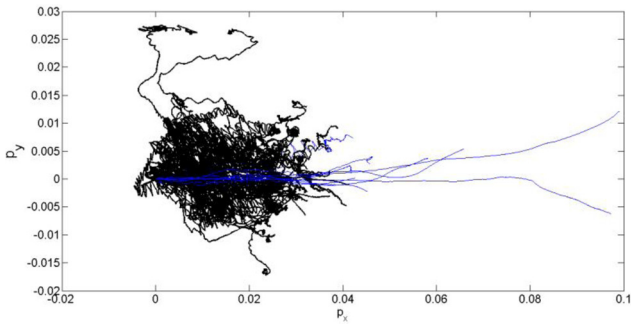

FIG. 5. Proton trajectories in momentum space in the simulation. P_x and P_y are normalized proton longitudinal and transverse momentum, respectively. The blue lines correspond to the $E > 0.8$ MeV protons, while the black lines to the $E < 0.8$ MeV protons. $E < 0.8$ MeV protons have much higher transverse momentums than that for $E > 0.8$ MeV protons.

Therefore, the counts of the $E > 0.8$ MeV protons are outstanding in the spectrum.

In previous experiments by Robinson *et al.*,[15] a quasi-monoenergetic proton peak is observed within a collection angle of 0.5 mrad in the target normal direction by using ultrathin nm-thick targets. The focusing effect of the self-generated magnetic field near the target center is responsible for the quasi-monoenergetic peaks. While, for μm-thick targets no monoenergetic feature is observed in the target normal. In our experiments, we have observed modulated spectral peaks off target normal direction for micron-thick targets. This indicates that by tuning the target thickness and laser parameters, one could make protons at specific energies dominant at certain angles.

IV. CONCLUSIONS

We have observed proton beams with spectral peaks presented in off-target normal direction in the interactions of femtosecond laser pulses with micron-thickness foil targets. Our PIC simulations show that a 100–1000 T toroidal magnetic field is generated at the rear target surface. The field can deflect most of protons, particularly for those with relatively low energy protons, consequently generating modulated spectral peaks. The peaks may be optimized by controlling the self-generated magnetic field through changing laser and target conditions.

ACKNOWLEDGMENTS

This work was supported by National Basic Research Program of China (Grant No. 2013CBA01501) and the National Nature Science Foundation of China (Grant Nos. 11375262 and 11135012).

[1]M. Borghesi, D. H. Campbell, A. Schiavi, M. G. Haines, O. Willi, A. J. MacKinnon, P. Patel, L. A. Gizzi, M. Galimberti, R. J. Clarke, F. Pegoraro, H. Ruhl, and S. Bulanov, Phys. Plasmas **9**, 2214 (2002).
[2]M. Roth, T. E. Cowan, M. H. Key, S. P. Hatchett, C. Brown, W. Fountain, J. Johnson, D. M. Pennington, R. A. Snavely, S. C. Wilks, K. Yasuike, H. Ruhl, F. Pegoraro, S. V. Bulanov, E. M. Campbell, M. D. Perry, and H. Powell, Phys. Rev. Lett. **86**, 436 (2001).
[3]S. V. Bulanov and V. S. Khoroshkov, Plasma Phys. Rep. **28**, 453 (2002).

[4]K. W. D. Ledingham, P. McKenna, and R. P. Singhal, Science **300**, 1107 (2003).
[5]A. Henig, S. Steinke, M. Schnürer, T. Sokollik, R. Hörlein, D. Kiefer, D. Jung, J. Schreiber, B. M. Hegelich, X. Q. Yan, J. Meyer-ter-Vehn, T. Tajima, P. V. Nickles, W. Sandner, and D. Habs, Phys. Rev. Lett. **103**, 245003 (2009).
[6]L. Yin, B. J. Albright, B. M. Hegelich, K. J. Bowers, K. A. Flippo, T. J. T. Kwan, and J. C. Fernández, Phys. Plasmas **14**, 056706 (2007).
[7]A. Henig, D. Kiefer, M. Geissler, S. G. Rykovanov, R. Ramis, R. Hörlein, J. Osterhoff, Z. Major, L. Veisz, S. Karsch, F. Krausz, D. Habs, and J. Schreiber, Phys. Rev. Lett. **102**, 095002 (2009).
[8]B. M. Hegelich, I. Pomerantz, L. Yin, H. C. Wu, D. Jung, B. J. Albright, D. C. Gautier, S. Letzring, S. Palaniyappan, R. Shah, K. Allinger, R. Hörlein, J. Schreiber, D. Habs, J. Blakeney, G. Dyer, L. Fuller, E. Gaul, E. Mccary, A. R. Meadows, C. Wang, T. Ditmire, and J. C. Fernandez, New J. Phys. **15**, 085015 (2013).
[9]D. Haberberger, S. Tochitsky, F. Fiuza, C. Gong, R. A. Fonseca, L. O. Silva, W. B. Mori, and C. Joshi, Nat. Phys. **8**, 95–99 (2011).
[10]M. H. Xu, Y. T. Li, X. H. Yuan, Q. Z. Yu, S. J. Wang, W. Zhao, X. L. Wen, G. C. Wang, C. Y. Jiao, Y. L. He, S. G. Zhang, X. X. Wang, W. Z. Huang, Y. Q. Gu, and J. Zhang, Phys. Plasmas **13**, 104507 (2006).
[11]Y. Q. Cui, W. M. Wang, Z. M. Sheng, Y. T. Li, and J. Zhang, Phys. Plasmas **20**, 024502 (2013).
[12]B. M. Hegelich, B. J. Albright, J. Cobble, K. Flippo, S. Letzring, M. Paffett, H. Ruhl, J. Schreiber, R. K. Schulze, and J. C. Fernandez, Nature **439**, 441 (2006).
[13]H. Schwoerer, S. Pfotenhauer, O. Jackel, K.-U. Amthor, B. Liesfeld, W. Ziegler, R. Sauerbrey, K. W. D. Ledingham, and T. Esirkepov, Nature **439**, 445 (2006).
[14]T. Toncian, M. Borghesi, J. Fuchs, E. d'Humieres, P. Antici, P. Audebert, E. Brambrink, C. A. Cecchetti, A. Pipahl, L. Romagnani, and O. Willi, Science **312**, 410 (2006).
[15]A. P. L. Robinson, P. Foster, D. Adams, D. C. Carroll, B. Dromey, S. Hawkes, S. Kar, Y. T. Li, K. Markey, P. McKenna, C. Spindloe, M. Streeter, C.-G. Wahlström, M. H. Xu, M. Zepf, and D. Neely, New J. Phys. **11**, 083018 (2009).
[16]Z. H. Wang, C. Liu, Z. W. Shen, Q. Zhang, H. Teng, and Z. Y. Wei, Opt. Lett. **36**, 3194 (2011).
[17]Y. Zheng, L. N. Su, M. Liu, B. C. Liu, Z. W. Shen, H. T. Fan, Y. T. Li, L. M. Chen, X. Lu, J. L. Ma, W. M. Wang, Z. H. Wang, Z. Y. Wei, and J. Zhang, Rev. Sci. Instrum. **84**, 096103 (2013).
[18]F. Lindau, O. Lundh, A. Persson, P. McKenna, K. Osvay, D. Batani, and C.-G. Wahlström, Phys. Rev. Lett. **95**, 175002 (2005).
[19]G. Sarri, A. Macchi, C. A. Cecchetti, S. Kar, T. V. Liseykina, X. H. Yang, M. E. Dieckmann, J. Fuchs, M. Galimberti, L. A. Gizzi, R. Jung, I. Kourakis, J. Osterholz, F. Pegoraro, A. P. L. Robinson, L. Romagnani, O. Willi, and M. Borghesi, Phys. Rev. Lett. **109**, 205002 (2012).
[20]M. Chen, Z. M. Sheng, J. Zheng, Y. Y. Ma, and J. Zhang, Chin. J. Comput. Phys. **25**, 43 (2008).
[21]W. M. Wang, Z. M. Sheng, P. A. Norreys, M. Sherlock, R. Trines, A. P. L. Robinson, Y. T. Li, B. Hao, and J. Zhang, J. Phys.: Conf. Ser. **244**, 022070 (2010).